

# CHARACTERIZATION OF OIL–WATER PLUG RELATED FLOW IN SLIGHTLY INCLINED PIPES

KSHANTHI PERERA<sup>1</sup>, SABA MYLVAGANAM<sup>2</sup> & RUNE W. TIME<sup>1</sup>

<sup>1</sup>Department of Petroleum Engineering, University of Stavanger, Norway.

<sup>2</sup>Department of Electrical Engineering, Information Technology and Cybernetics,  
University College of Southeast Norway, Norway.

## ABSTRACT

Flow patterns in oil–water carrying pipes vary due to the flow characteristics, fluid properties and pipe inclination. For inclined pipes, the gravity component along the pipe influences the flow patterns. Plug flow (PF) is one special flow pattern that occurs in slightly upward inclined pipe-lines. Mineral oil–Exxsol D60 (viscosity = 1.6 mPa.s, density = 788 kg/m<sup>3</sup>) and water (viscosity = 1 mPa.s, density = 997 kg/m<sup>3</sup>) were used as test-fluids. A test matrix was carried out to determine the possible flow patterns that occur at upward pipe inclinations +1°, +3°, +5° and +6° for low mixture velocities (0.2–0.5 m/s), and at water-cut 0.9. The plug flow regime was found only for +5° and +6° inclinations, while no plug flow was noticed at +1° and +3° inclinations. Plug flow was found only for lower flow velocity and higher water-cuts. Plug flow patterns were identified both through visual observation and by means of high-speed video imaging. Two new flow patterns ‘oil droplet clusters in continuous oil and water (OC/O&W)’ and ‘distinct oil droplet clusters in water (D-OC/W)’ were introduced, and they occur around the plug flow regime. High-speed images were post-processed for determination of the oil–water interface and subsequently used to calculate the water hold-up. The time averaged water hold up decreased with increasing mixture velocity due to the decrease of oil–water slip as a result of increased degree of dispersion. The oil plugs entrained more droplets as mixture velocity was increased, leading to high-frequency fluctuations of volume fraction of the oil plugs. Hold-up increased with increasing inclination due to the onset of plug flow, which leads to increased slip. The pressure drop over the test section was measured, and the frictional pressure drops were calculated using average water hold-up values. The frictional pressure drop increased with increasing mixture velocity, due to increased mixing and subsequent increase of effective viscosity. The frictional pressure drop decreased with increased inclination due to the appearing of oil plugs and the drag reduction effect associated with the plug flow.

*Keywords:* flow patterns, frictional pressure drop, phase slip, plug flow, water hold-up

## 1 INTRODUCTION

The flow patterns in oil–water transportation pipelines can vary a lot, based on the flow rates, properties of oil and water, pipe diameter, pipe material, inclination, and etc. The flow patterns are important due to their influence on pressure fluctuations, phase slip, drag reduction, possibility of flow reversal and thus for flow control and safety purposes.

Only modest number of studies have been carried out on oil–water flow patterns in pipelines, compared to research on liquid–gas flows. Even less is done on inclined pipes. The increased momentum transfer and reduced buoyancy effects make liquid–liquid systems different from liquid–gas systems. Still, pipe inclination influences oil–water flow patterns, hold-up and slip between the phases.

Table 1 summarizes recent studies done on oil–water flow patterns classification for horizontal and near horizontal upward (+) inclined pipes for low-to-moderate viscous oil and water flow. According to the study of Trallero [1], (horizontal pipe, diameter: 50.13 mm,  $\mu_o / \mu_w: 29.6$ ,  $\rho_o / \rho_w: 0.85$ , T: 25.6°C) all resulted oil–water flow patterns can be classified into two basic categories, as segregated flow and dispersed flow. The segregated flow patterns are ‘stratified flow (ST)’ and ‘stratified and mixed interface (ST&MI)’. These are gravity

Table 1: Recent oil-water flow studies on positive and slightly inclined pipe flows for low viscous oil.

Study	$\mu$ (mPa.s) $\rho$ (kg / m <sup>3</sup> )	Flow conditions		Flow patterns
		$U_{\text{mix}}$ (m / s) and $\lambda_w$		
Alkaya [6] $\theta : 0^\circ, 0.5^\circ, 1^\circ, 2^\circ, 5^\circ$ D:50.8 mm P:1.4 bar T:35°C	$\mu_o : 12.9$ $\rho_o : 848$ $\mu_w : 0.72$ $\rho_w : 994$	$U_{\text{mix}} : 0.025 - 1.75$ $\lambda_w : 0 - 1$		ST, ST&MI, Do/w&w, Dispersed water in oil &oil(Dw/o&o), Dw/ o&Do/w, Dw/o, Do/w
Lum <i>et al.</i> [4] $\theta : 0^\circ, 5^\circ$ D:38 mm	$\mu_o : 5.5$ $\rho_o : 828$ $\mu_w : 0.993$ $\rho_w : 998$	$U_{\text{mix}} : 0.7 - 2.5$ $\lambda_w : 0.1 - 0.9$		SW, Dual continuous (DC), Do/w, Dw/o
Lum <i>et al.</i> [5] $\theta : 0^\circ, 10^\circ$ D:38 mm	$\mu_o : 5.5$ $\rho_o : 828$ $\mu_w : 0.993$ $\rho_w : 998$	$U_{\text{mix}} : 0.7 - 2.5$ $\lambda_w : 0.1 - 0.9$		SW, Dual continuous (DC), Do/w, Dw/o, PF
Rodriguez and Oliemans [2] $\theta : 0^\circ, 1^\circ, 2^\circ, 5^\circ$ D:82.5 mm	$\delta : 7.5$ $\rho_o : 830$ $\mu_w : 0.8$ $\rho_w : 1060$	$U_{\text{mix}} : 0.04 - 5.55$ $\lambda_w : 0.1 - 0.9$		ST, ST&MI, Do/w&w, Dw/o&Do/w, Do/w, Dw/o, SW
Kumara <i>et al.</i> [3] $\theta : 0^\circ, 1^\circ, 5^\circ$ D:56.3 mm	$\mu_o : 1.64$ $\rho_o : 790$ $\mu_w : 1$ $\rho_w : 1060$	$U_{\text{mix}} : 0.25 - 1.5$ $\lambda_w : 0.025 - 0.975$		ST, ST&MI, Do/w&w, Dw/o&Do/w, Do/w, Dw/o, SW,PF

Here  $\theta$ :pipe inclination, D:pipe diameter,  $\mu_o$ :oil viscosity,  $\mu_w$ :water viscosity,  $\rho_o$ :oil density,  $\rho_w$ :water density,  $U_{\text{mix}}$ :mixture velocity,  $\lambda_w$ :input water-cut

dominated and occur at low oil and water superficial velocities. ST flow has a smooth interface with no mixing and the oil and water flow as layers. Increase of the flow rates lead to transition from ST flow to ST&MI due to increased turbulence, which eventually leads to interfacial mixing of oil and water phases with droplet formation. These droplets mostly stay at the interface since the gravity-buoyancy forces still dominate over the spreading effect of turbulent dispersion. Dispersed flow can be sub-classified into water-dominated flow and oil-dominated flow. Dispersed flow occurs at moderate to higher superficial velocities when turbulence in the oil and water layers becomes sufficiently high. When the water-cut ( $\lambda_w$ ) is high, the flow is water dominated and the continuity of the oil layer is disrupted by the water vortices and break the oil layer into droplets. Depending on the flow velocity and the balance of gravity versus turbulence, the droplets can be localized toward the top of the pipe or more evenly distributed across the pipe cross-section. This leads to ‘dispersed oil in water and water (Do/w&w)’ or ‘dispersed oil in water (Do/w)’ flow patterns. Vice versa when  $\lambda_w$  is lower so that the system becomes oil dominated, the flow patterns become ‘dispersed water in oil and oil in water (Dw/o&Do/w)’ or ‘dispersed water in oil (Dw/o)’. The flow pattern

maps of Rodriguez and Oliemans [2], Kumara *et al.* [3], describe the same flow patterns as Trallero [1] for horizontal pipes. However, Rodriguez and Oliemans [2] reports ‘caterpillar’ waves at +2° inclination, and Kumara *et al.* [3] describes clear stratified wavy region at +5° inclination at  $U_{mix}:0.25$  m/s and  $\lambda_w: 0.25\text{--}0.9$ . Also, Lum *et al.* [4, 5] report SW flow for inclinations +5° and +10°. Kumara *et al.* [3] reports clear intermittent oil plugs in water at +5°,  $U_{mix}:0.25$  m/s and  $\lambda_w \geq 0.925$  and Lum *et al.* [5] noticed the same in +5° and +10° for  $U_{mix}:0.6\text{--}1.0$  m/s and  $\lambda_w: 0.7\text{--}0.9$ . Very few researchers report on oil plugs in water and the knowledge regarding to these oil-plugs is rather scanty. Therefore, this paper aims on specifically study on oil plugs those occur in upward (+) inclined pipes.

## 2 EXPERIMENTS

Mineral oil (Exxsol D60) and water are the test fluids for this study. Their properties are given in Table 2.

### 2.1 Experimental setup

The multiphase flow facility at University College of Southeast Norway was used for performing the experiments. A sketch of the flow facility is shown in Fig. 1.

Oil and water are pumped from the storage tanks T100 and T101 using the five pumps P100, P101, P102, P103 or 104 in order to provide the desired mixture velocity and the water-cut. P100 is the main oil pump for high oil flow rates and P101 is the main water pump for high water flow rates. The other pumps P102, 103 or 104 can be used for either oil or water according to need. The flow controllers FC-108 and FC-113 are used for the pumps P100 and P101. FC-177 and FC-168 are important flow controllers to adjust the desired oil and water flow rates through the pumps P100 and P101. The flow rate and the density of each liquid is measured with the Coriolis flowmeters FT-110, FT-115, FT-109B and FT-114B, based on the range of flow rates involved. FT-109B and FT-114B are for small flow rates. The flow meters FT-114A and FT-109A monitor the water or oil flow through the bypass lines of the Coriolis flowmeters FT-114B and FT-109B. The oil and water streams were combined using a Y-junction to minimize interfacial mixing at the entry point to the test section. A long, thin horizontal separation plate (35 cm) was inserted at the Y junction so that the oil and water could flow as layers into the test section. The test section is a 15 m long stainless steel pipe with inner diameter of 56.3 mm. It is inclinable 6° downwards and upwards. Two differential pressure transducers PDT-120 and PDT-121 were installed across the length of the test section. Visual observation and high-speed video recordings of the oil–water flow were facilitated by a transparent test section. After flowing through the test section, the oil–water flow enters the pre-separator tank and subsequently to the separator. After separation, oil and water is returned to the tanks for continuous circulation. A LabVIEW-based control program was used for monitoring and operating the flow facility.

Table 2: Properties of oil and water relevant to this study at 1 atm.

Properties	Water	Oil (Exxsol D60)
Density @ 20°C [kg/m <sup>3</sup> ]	997	788
Viscosity @ 20°C [mPa s]	1	1.6
Surface tension @ 20°C [mN/m]	72	25

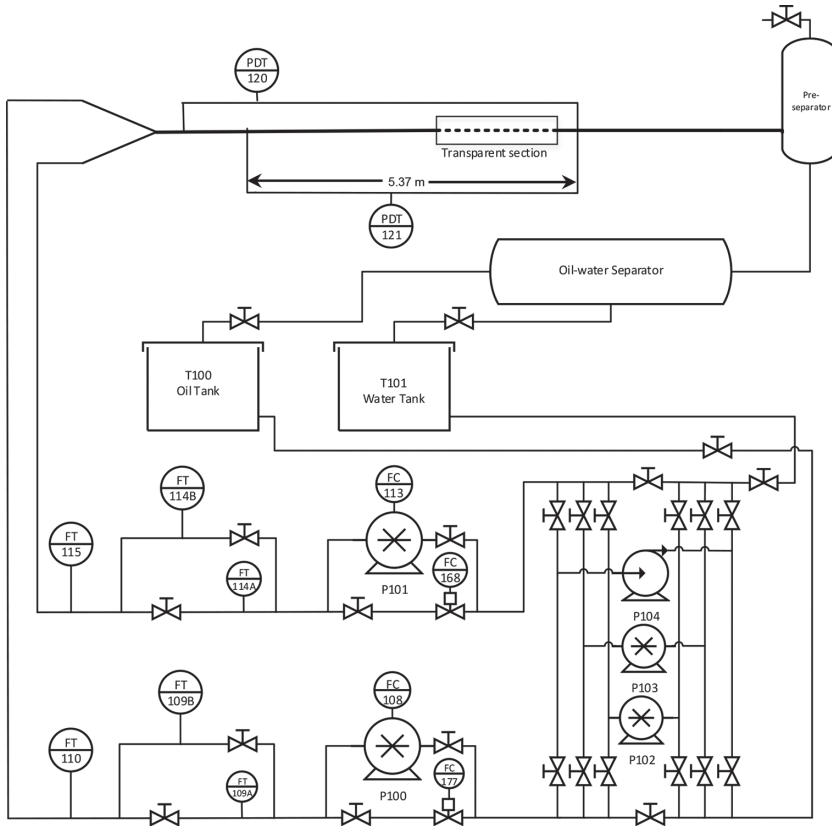


Figure 1: Simplified sketch of the oil–water flow facility.

## 2.2 Measurement procedure

The experiments were conducted at  $+1^\circ$   $+3^\circ$   $+5^\circ$   $+6^\circ$  inclinations. The mixture velocities were 0.2–0.5 m/s and the water-cut, 0.9. Here, the mixture velocity  $U_{\text{mix}}$  is defined by eqn (1) and the water-cut  $\lambda_w$ , is defined by eqn (2).  $Q_o$  and  $Q_w$  are the oil and water flow rates in  $\text{m}^3/\text{s}$ , and  $A$  is the cross-sectional area of the pipe in  $\text{m}^2$ .

$$U_{\text{mix}} = \frac{Q_o + Q_w}{A} \quad (1)$$

$$\lambda_w = \frac{Q_w}{Q_o + Q_w} \quad (2)$$

The flow was allowed to stabilize for at least 10 min before measurement of each flow pattern. The flow patterns were identified and recorded by visual observations and from high-speed video imaging.

### 2.2.1 Hold-up measurements

The water ‘hold-up’ is defined as the fraction of the pipe cross-sectional area occupied by the water at a given position [7]. The ratio between the in-situ oil-to-water velocities is known as the slip ratio.

Since the water fraction is time dependent for flow patterns such as SW and PF, the time averaged local volume fraction is considered as the representative hold-up.

High-speed images (from Photron FASTCAM camera) were post-processed for estimation of hold-up values. The oil–water interface at a certain pixel column (i.e. along a vertical slice in the image, one pixel wide) was detected via image analysis. This enabled determination of the time varying oil–water interfacial height. The oil–water interphase was assumed to be planar at each instant. Thus, the cross-sectional pipe area occupied by water could be calculated by a geometrical relation as a function of the interfacial height. The frame rate was 500 Hz and the images were recorded for 15 s.

However, the hold-up prediction method can be erroneous or at least have some uncertainty. One is due to the assumption of flat oil–water interface. In reality, the oil–water interface can be slightly curved or inclined due to the presence of plug. For this reason, the method may at times underpredict the water hold-up and subsequently the frictional pressure drop as well. In addition, the interface detection considered the brightest pixel along the image columns, as the interface. Again, due to optical effects, the brightest pixel might not necessarily be the pixel, which represents the actual interface in the image frame.

### 2.2.2 Pressure drop measurements

A ‘Rosemount-3051’ differential pressure transmitter (measurement range of 0–50 mbar) measured the total pressure drop over the test section. The connection pipes to the pressure transmitter were filled with water.

For the inclined pipes, the measured pressure drop  $\Delta P_f/\Delta L$  is the sum of frictional pressure drop  $\Delta P_f/\Delta L$ , pressure drop due to elevation and the acceleration. Assuming negligible contribution of acceleration on oil–water systems, the frictional pressure drop can be found straightforward by subtracting the impact of hydrostatics associated with the oil–water mixture density in the pipe and water which is used in the connection pipes. This is given in eqn (3).

$$\frac{\Delta P_f}{\Delta L} = \frac{\Delta P_t}{\Delta L} - (\rho_w - \rho_{mix}) g \sin \theta \quad (3)$$

Here,  $\Delta L=5.37$  m, is the distance between the inlets to the PDT-121 sensor,  $g$  is the gravitational acceleration,  $\theta$  is the inclination angle with respect to the horizontal level,  $\rho_w$  and  $\rho_{mix}$  are density of water and the oil–water mixture, respectively.

The mixture density ( $\rho_{mix}$ ) is calculated using the water hold-up measurements as shown in eqn (4).

$$\rho_{mix} = \rho_w H + \rho_o (1 - H) \quad (4)$$

Here,  $H$  is the running time averaged water hold-up calculated by image analysis. The accuracy of the pressure measurements is  $\pm 0.1\%$  of the measurement range, which is  $\pm 0.05$  mbar.

## 3 RESULTS AND DISCUSSION

### 3.1 Oil plugs occurrence at different inclinations and mixture velocities

PF is a time-dependent flow pattern. In this paper, the oil plugs are defined so that they have clearly identifiable head, which may or may not contain droplets, and a clearly identifiable tail. The flow pattern map as shown in Fig. 2 summarizes the observed flow-details relevant to

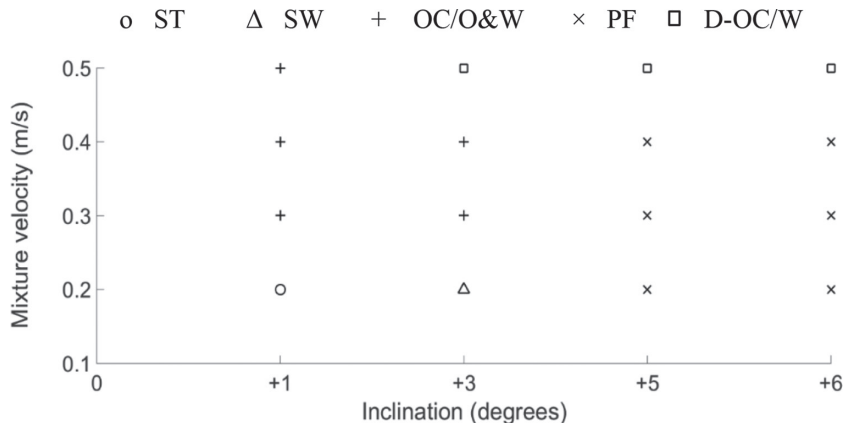


Figure 2: Flow pattern map for low velocity region for upwardly inclined flows at  $\lambda_w = 0.9$ .

the test matrix. For horizontal oil–water flows, there is no effect from gravity except for the cross-sectional wave behavior and Kelvin-Helmholtz wave instabilities. Else, mainly the fluid viscosities, and the flow velocity determine the flow patterns for a given input water-cut. However, when it comes to inclined flows the gravity effects matter and becomes more and more significant with the increase of inclination. As represented by flow pattern map in Fig. 2, the plug flow (PF) occurred for  $\theta = +5^\circ$  and  $+6^\circ$ . At  $U_{\text{mix}} = 0.2 \text{ m/s}$ , the flow has changed from stratified smooth (ST- see Fig. 3(a)) to stratified wavy (SW- see Fig. 3(b)) and then to plug flow (PF-see Fig. 4) with the increased inclination. The oil–water flow at near horizontal flow ( $+1^\circ$ ) stays stratified due to the lower oil and water superficial velocities within the phase and

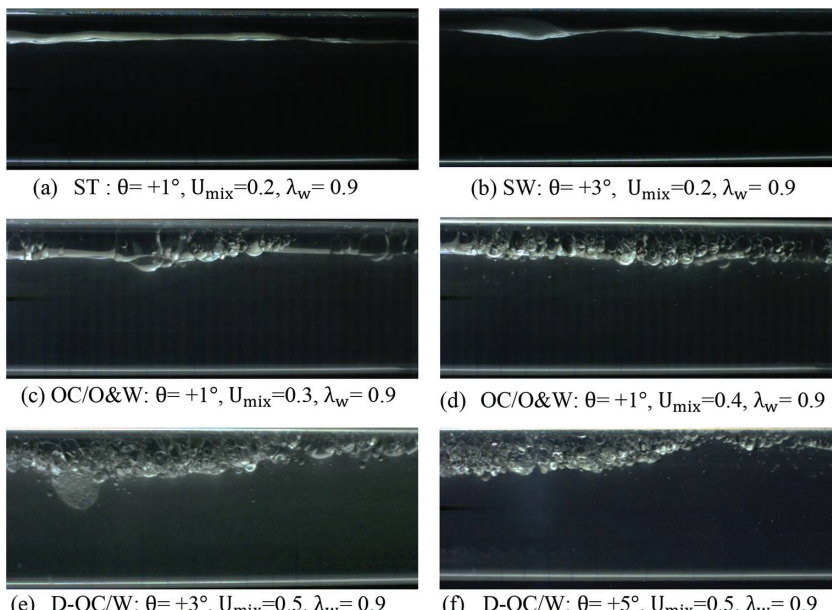


Figure 3: Different flow regimes occurring around the plug flow region ( $U_{\text{mix}}$  in m/s).

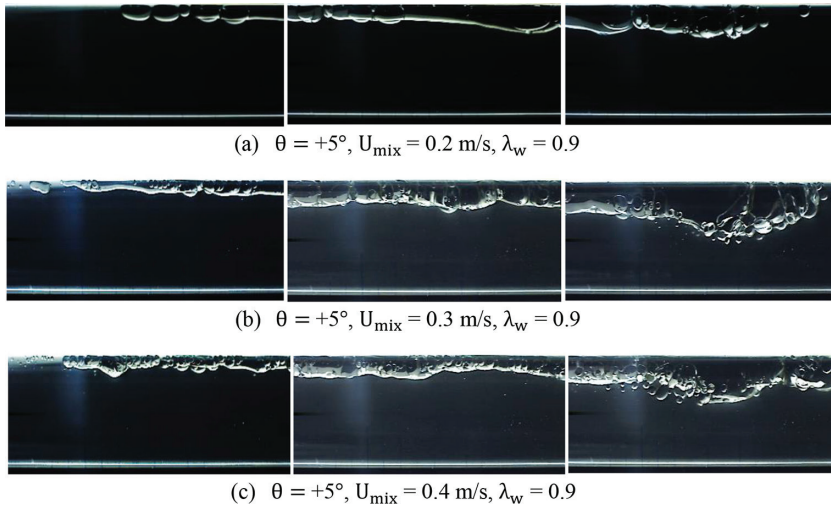


Figure 4: Plug flow at different mixture velocities:  $\theta = +5^\circ$  and  $\lambda_w = 0.9$ .

less gravity effects prevent the interfacial mixing. With inclinations steeper than  $+3^\circ$ , the flow is more influenced by axial gravity effects. Phase slip is then associated with oil flowing faster than the water. As a result, the water hold-up increases with increasing inclination as indicated in Fig. 7. Due to the phase slip with oil flowing faster than the water, waves are created (SW). Further increase in inclination ( $+5^\circ$  and  $+6^\circ$ ), leads to higher shear, and more breakup of the oil phase via instability of the wavy structure. The higher slip leads to further decrease in-situ oil volume fraction, and also change of flow regime into plug flows (PF). The features of the PF regime also vary according to the mixture velocity and the inclination. Higher mixture velocity causes more and more liquid vortices due to increased turbulence. This leads to mutual droplet entrainment of one phase into the other. At given oil–water fractions, this may lead to phase inversion, which eventually results in dispersed oil in water and water (Do/w&w) flow regime. For very high water-cuts, the flow ends up with dispersed oil in water (Do/w) flow. Turbulence leads to more mixing of oil water phases and again leads to higher droplet concentration. Two new flow regimes were identified around the plug flow regime:

1. Oil droplet clusters appear periodically in the continuous oil layer, and there is a clear water layer underneath – (OC/O&W)-see Fig. 3(c) and (d).
2. Distinct oil droplet clusters which have marginal differences with dispersed oil in water and water (Do/w&w) flow regime-(D-OC/W) – see Fig. 3(e) and (f).

This cannot be defined as ‘dispersed oil in water and water’ flow regime, since they remain as oil droplets bounded to each other, but not dispersed in water.

Table 3 describes the features of the plugs occurring at different flow conditions for inclination angle  $\theta = +5^\circ$  and  $+6^\circ$ .

### 3.2 Water hold-up

Figure 5 shows the time varying water hold-up obtained via oil–water interface detection of high-speed images for  $\theta = +5^\circ$  and  $\lambda_w = 0.9$  at different mixture velocities. It explains the flow

Table 3: Plug flow details for inclination angles  $\theta = +5^\circ$  and  $\theta = +6^\circ$ .

$U_{\text{mix}}$ (m/s)	Flow patterns ( $\theta = +5^\circ$ , $\lambda_w = 0.9$ )
0.2	Clearly distinct intermittent plugs in clear water, with head and tail. Sometimes the tail consists of huge egg-shaped droplets. No dispersed tiny droplets are seen – (PF) – see Fig. 4(a)
0.3	Clearly distinct oil plugs with some dispersed droplets inside. Long and the oil layer height changes significantly along the plug length– (PF) – see Fig. 4(b)
0.4	Distinct oil plugs with dispersed oil droplets inside. Comparatively thin, with long tail in comparison to plug head – (PF) – see Fig. 4(c)
0.5	Distinct clusters made with oil droplets in water-(D-OC/W)

$U_{\text{mix}}$ (m/s)	Flow patterns ( $\theta = +6^\circ$ , $\lambda_w = 0.9$ )
0.2	Clearly intermittent plugs, much shorter (PF)
0.3	Clearly distinct bubbly plugs. However, not so smooth. Heavy wide plug head. Large variation of oil layer height across the plug – (PF)
0.4	Nearly continuous thin oil plugs with oil droplets. No large variations in oil layer height along the plug – (PF)
0.5	Distinct oil droplet clusters in water (D-OC/W)

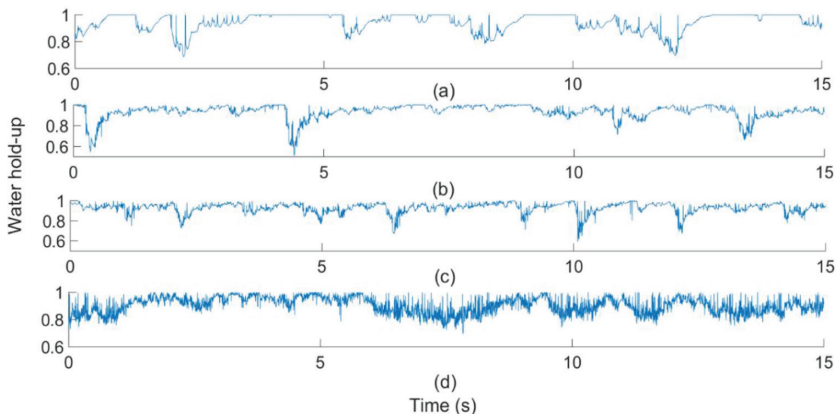


Figure 5: Time series of values water hold-up based on high speed images at  $\theta: +5^\circ$ ,  $\lambda_w: 0.9$ .  
 (a)  $U_{\text{mix}}: 0.2 \text{ m/s}$ ; (b)  $U_{\text{mix}}: 0.3 \text{ m/s}$ ; (c)  $U_{\text{mix}}: 0.4 \text{ m/s}$ ; (d)  $U_{\text{mix}}: 0.5 \text{ m/s}$ .

features of PF described in Table 3 and illustrated in Fig. 4 up to some extent. Higher hold-up variation with increasing velocity is connected to increased amount of oil droplets associated with the oil-flow. The intermittent feature of the plugs are shown by hold-up value 1, which prevails for short period of time where the whole pipe cross-section is filled with water until the next appears.

As indicated in Fig. 6, the average water hold-up decreases with increasing mixture velocity, due to the reduction of slip associated with increasing mixing and droplet dispersion.

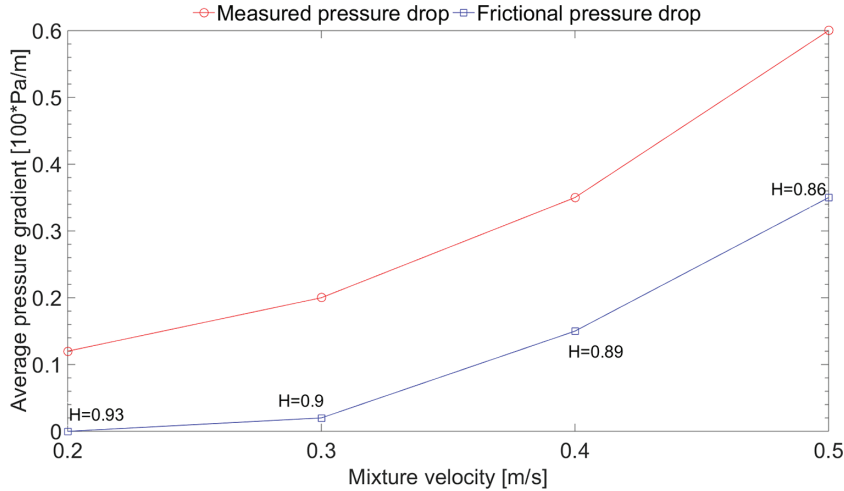


Figure 6: Time average pressure gradient at different mixture velocities for  $\theta : +5^\circ$ ,  $\lambda_w : 0.9$ .

\*Time average water hold-up (H) corresponding to each data point is mentioned

\*The average pressure gradient for single phase water at  $\theta : +5^\circ$ , velocity 0.4 m/s is 50 Pa/m

Lum *et al.* [5] has obtained the decrease of water hold-up (reduced slip ratio) with increasing mixture velocity for PF regime.

As indicated in Fig. 7, the water hold-up generally increases with increasing pipe inclination due to the increased slip. The increased hold-up (and increased slip) is attributed to appearing of PF at  $+5^\circ$  and  $+6^\circ$  and Lum *et al.* [5] and Kumara *et al.* [7] also report the increased slip as a result of PF flow regime.

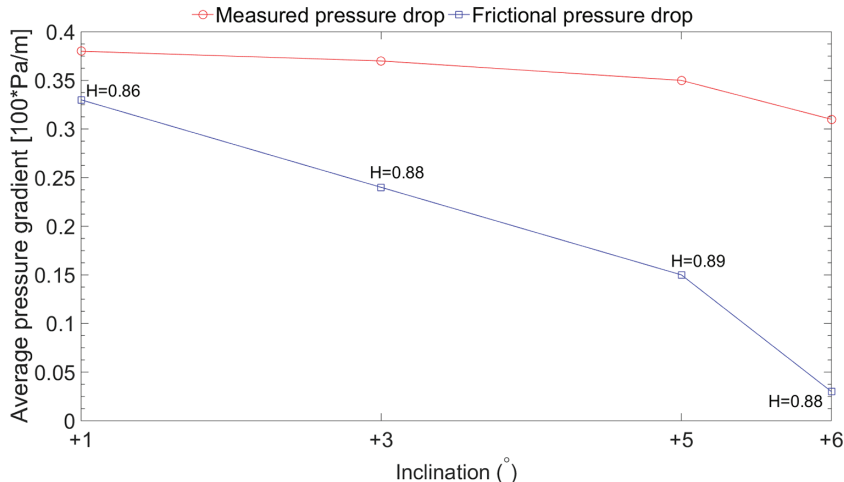


Figure 7: Time average pressure gradient at different inclinations,  $U_{\text{mix}} : 0.4$  m/s,  $\lambda_w : 0.9$ .

(Average pressure gradient measured for water at  $\theta : 0^\circ$ ,  $\lambda_w : 1$  is 37 Pa/m)

### 3.3 Frictional pressure drop and the mixture velocity at $\theta = +5^\circ$ and $\lambda_w = 0.9$

6 shows, increment of frictional pressure drop with increment of mixture velocities. Lum *et al.* [5], Abduvayt *et al.* [8] and Kumara *et al.* [7] also report the same trend. For higher water-cut cases as  $\lambda_w = 0.9$ , the flow is water dominant. Increased mixture velocity leads to higher turbulence within the water layer and causes the water vortices to get in to the oil layer, thus breaking up the oil into more droplets. This leads to increased effective viscosity and subsequently higher pressure drop. Kumara *et al.* [7] describes phase inversion which leads to a peak in frictional pressure drop at water-cut around 0.9 for mixture velocities 0.5 m/s, and 1.0 m/s. This peak in frictional pressure gradient is shifted toward lower water-cuts at higher velocities and it is not significant in lower mixture velocities.

In this current study, we observe a gradual increase of frictional pressure drop toward phase inversion. But from the high-speed video images the phase inversion is not yet reached at  $U_{\text{mix}} = 0.5$  m/s for  $\lambda_w = 0.9$  and is expected to occur at much higher velocity. For horizontal flows, the phase inversion occurs already at these values with the flow regime being ‘Dispersed oil in water and water’ (Do/w&w) at  $U_{\text{mix}} = 0.5$  m/s for  $\lambda_w = 0.9$ . Here, the obtained frictional pressure gradient was 70 Pa/m.

### 3.4 Frictional pressure drop and the pipe inclination at $\lambda_w = 0.9$ and $U_{\text{mix}} = 0.4$ m/s

Figure 7 shows a gradual decrease of frictional pressure drop with increasing inclination. Amundsen [9] measured lower normalized frictional pressure gradient for the upwardly inclined pipe flow than the horizontal for all three considered inclinations,  $+1^\circ$ ,  $+5^\circ$  and  $+10^\circ$ . Lum *et al.* [5] also measured the frictional pressure drop lower than that of horizontal for  $+5^\circ$  at 1.0 m/s especially for higher input water fractions. So, this study confirms the same trend. A reduction in frictional pressure drop is observed with the appearance of plugs. On the other hand, the two-phase frictional pressure drop is lower for all the inclinations than that of the horizontal single phase water measured at mixture velocity 0.4, which is 37 Pa/m. Lum *et al.* [5] also reported less two-phase pressure gradients than that of single phase water at  $+5^\circ$  inclination and  $U_{\text{mix}} = 1.0$  m/s. The reduced pressure drop with increasing inclination can be attributed to the drag reduction effect, which might occur due to the appearance of oil-plugs associated with droplets.

When measuring the two phase pressure gradients, the uncertainties of the measurements become higher especially for the upwardly inclined pipe flows since the gravitational pressure forces balances the frictional pressure forces and the measured pressure drop becomes closer to zero [9].

## 4 CONCLUSION

Oil–water two phase flow was studied for the low mixture velocity region ( $U_{\text{mix}} = 0.2$ – $0.5$  m/s) at  $\lambda_w = 0.9$  for upwardly inclined pipes ( $\theta = +1^\circ$ ,  $+3^\circ$ ,  $+5^\circ$ ,  $+6^\circ$ ). The flow patterns were determined and captured through high-speed video imaging at a rate of 500 Hz. A flow pattern map was generated to summarize the observed flow features. Two new flow regimes, ‘Oil droplet clusters in continuous oil and water (OC/O&W)’ and ‘Distinct-oil droplet clusters in water (D-OC/W)’ were defined in addition to the stratified smooth (ST), stratified wavy (SW) and plug flow (PF) regimes.

The water hold-up was determined through detection of the oil–water interface level in high-speed images and then used to calculate the water cross-sectional area in the pipe, under

the assumption of a flat interface between oil and water. This was done automated using Matlab for each image frame, and thus as a function of time. The water hold-up decreased with increasing mixture velocities due to the reduction of slip because of increased degree of dispersion. The water hold-up increased with increasing inclination due to the increased slip that occurs in the presence of plug flow. The hold-up values may at times be underpredicted compared to the real water hold-up since a flat oil–water interface is assumed for the upwardly curved interface present in the real flows. As a result, this may underpredict the estimated frictional pressure drops as well.

The pressure drop along the test section was measured using a Rosemount-3051 DP transmitter and the average frictional pressure drops were calculated using the time average water hold-up values obtained from high-speed image analysis. The frictional pressure drop increased with increasing mixture velocity as expected. Also increasing inclination reduced the frictional pressure drop due to the appearance of plug flow and possible subsequent drag reduction.

It could be worthwhile to perform a finer test matrix around the plug flow regime to identify exact boundaries of onset of PF and the transition. This would enhance the knowledge on the effects of plug flow on frictional pressure drop, phase slip and drag reduction, which are practically important aspects in process control and safety operations.

#### ACKNOWLEDGEMENTS

The authors gratefully acknowledge Professor Morten C. Melaaen, Dean Faculty of Engineering, Vice Dean Randi T. Holta, and Associate Professor Amaranath Sena Kumara of USN, for providing the opportunity and the test facilities to perform this research. We appreciate the help provided by Docent Finn Aakre Haugen in providing us with the data logging and control programs and updating them in conjunction with the measurements done in the multi-flow testing facilities of USN. Sincere thanks are extended to Dr.Chaminda Pradeep and the laboratory engineer, Fredrik Hansen for their great supports in assisting with the experiments and Dr. Andre. V. Gaathaug for providing the high-speed camera facilities.

We are grateful to the Government of Norway (Kunnskapsdepartementet - KD) and the ‘Statoil Akademia-UiS’ cooperation project for funding and providing support to this research.

#### REFERENCES

- [1] Trallero, J., Sarica, C. & Brill, J., A study of oil–water flow patterns in horizontal pipes. *SPE Production & Facilities*, **12**(3), pp. 165–172, 1997.  
<https://doi.org/10.2118/36609-pa>
- [2] Rodriguez, O. & Oliemans, R., Experimental study on oil–water flow in horizontal and slightly inclined pipes. *International Journal of Multiphase Flow*, **32**(3), pp. 323–343, 2006.  
<https://doi.org/10.1016/j.ijmultiphaseflow.2005.11.001>
- [3] Kumara, W.A.S., Halvorsen, B.M. & Melaaen, M.C., Pressure drop, flow pattern and local water volume fraction measurements of oil–water flow in pipes. *Measurement Science and Technology*, **20**(11), p. 114004, 2009.  
<https://doi.org/10.1088/0957-0233/20/11/114004>
- [4] Lum, J.Y.L., Lovick, J. & Angeli, P., Low Inclination Oil-water Flows. *The Canadian Journal of Chemical Engineering*, **82**(2), pp. 303–315, 2004.  
<https://doi.org/10.1002/cjce.5450820211>

- [5] Lum, J.L., Al-Wahaibi, T. & Angeli, P., Upward and downward inclination oil–water flows. *International Journal of Multiphase Flow*, **32**(4), pp. 413–435, 2006.  
<https://doi.org/10.1016/j.ijmultiphaseflow.2006.01.001>
- [6] Alkaya, B., *Oil-water flow patterns and pressure gradients in slightly inclined pipes*, Master Thesis. University of Tulsa, Oklahoma, 2000.
- [7] Kumara, W.A.S., Halvorsen, B.M. & Melaaen, M.C., Single-beam gamma densitometry measurements of oil–water flow in horizontal and slightly inclined pipes. *International Journal of Multiphase Flow*, **36**(6), pp. 467–480, 2010.  
<https://doi.org/10.1016/j.ijmultiphaseflow.2010.02.003>
- [8] Abduvayt, P., Manabe, R., Watanabe, T. & Arihara, N., Analysis of Oil-Water Flow Tests in Horizontal, Hilly-Terrain, and Vertical Pipes. In *SPE Annual Technical Conference and Exhibition*, 2004.  
<https://doi.org/10.2118/90096-ms>
- [9] Amundsen, L., *An experimental study of oil-water flow in horizontal and inclined pipes*, PhD Thesis, Norwegian University of Science and Technology, Norway, 2011.